NASA Technical Paper 1162

Temperature Distributions of a Cesium-Seeded Hydrogen-Oxygen Supersonic Free Jet

Shih-Ying Wang and J. Marlin Smith

FEBRUARY 1978

NASA

NASA Technical Paper 1162

Temperature Distributions of a Cesium-Seeded Hydrogen-Oxygen Supersonic Free Jet

Shih-Ying Wang and J. Marlin Smith
Lewis Research Center
Cleveland, Ohio

National Aeronautics
and Space Administration

**Scientific and Technical
Information Office**

1978

TEMPERATURE DISTRIBUTIONS OF A CESIUM-SEEDED HYDROGEN-OXYGEN SUPERSONIC FREE JET

by Shih-Ying Wang* and J. Marlin Smith

Lewis Research Center

SUMMARY

Radial distributions of temperature were determined spectroscopically in a cesium-seeded, hydrogen-oxygen plasma jet. The plasma was generated at combustion chamber pressures ranging from 0.5 to 2.0 megapascals and for various seed ratios (1 to 10 percent). The plasma was observed as the atmospheric exhaust from a NASA Lewis Mach 2 rocket test facility.

Transverse profiles of the absolute integrated intensity were measured with the optically thin CsI lines (0.5664 and 0.5636 μm) at a range of axial positions downstream of the 5-centimeter-diameter combustor-nozzle exit. Radial profiles of the emission coefficient were obtained from the measured transverse profiles of intensity by Abel inversion. Temperatures were then determined from the emission coefficients for conditions of local thermodynamic equilibrium using particle densities generated by a two-dimensional free jet computer program. Temperature results show the inherent effects of compression and expansion pressure waves characteristic of a free jet exiting from a supersonic nozzle.

INTRODUCTION

Optical spectroscopy is frequently used to determine particle temperatures and densities in dense plasmas because it is one of the few diagnostic methods which does not disturb the plasma. The development of such optical diagnostics is therefore highly desirable for advanced combustion systems where physical probes cannot survive due to the severity of the environment, or where their sizes severely disturb the flow.

This report discusses the spectroscopic measurement of emission intensities in a

---

*National Research Council - National Aeronautics and Space Administration Research Associate.

cesium-seeded, hydrogen-oxygen plasma free jet with a primary emphasis on determining the radial temperature profiles in order to assess the spatial uniformity of injected seed.

EXPERIMENTAL APPARATUS AND PROCEDURE

A rocket test facility (ref. 1) at the NASA Lewis Research Center is being used to generate a combustion plasma. This plasma is a stoichiometric mixture of hydrogen and oxygen seeded with an aqueous solution of cesium hydroxide (CsOH) (75 percent CsOH, 25 percent H_2O by weight) that is atomized in the oxygen flow line before entering the combustion chamber. The plasma is accelerated in a Mach 2 nozzle and then expanded to atmosphere at the 5-centimeter-diameter exit. The sequence of gas injection and ignition is controlled by a repeat cycle programmer to cover the running time from 5 to 20 seconds. Test-condition data such as flow rates and pressures are automatically sampled and processed by an IBM 360 computer; they are also recorded on a high speed oscillograph. Detection of the cesium spectral lines is accomplished with a scanning monochromator having a reciprocal linear dispersion of 1.6 nanometer per millimeter. Two optically thin CsI lines (0.5664 and 0.5636 μm) and a continuum at 0.5704 micrometer (for continuum correction) are found appropriate for absolute intensity measurement (see appendix A).

The optical system is shown in figure 1. Plasma radiation first strikes the stationary mirror, which is inclined at a 45° angle to both the optical and vertical axes. A second mirror is mounted below the stationary mirror on a motor-driven rotating

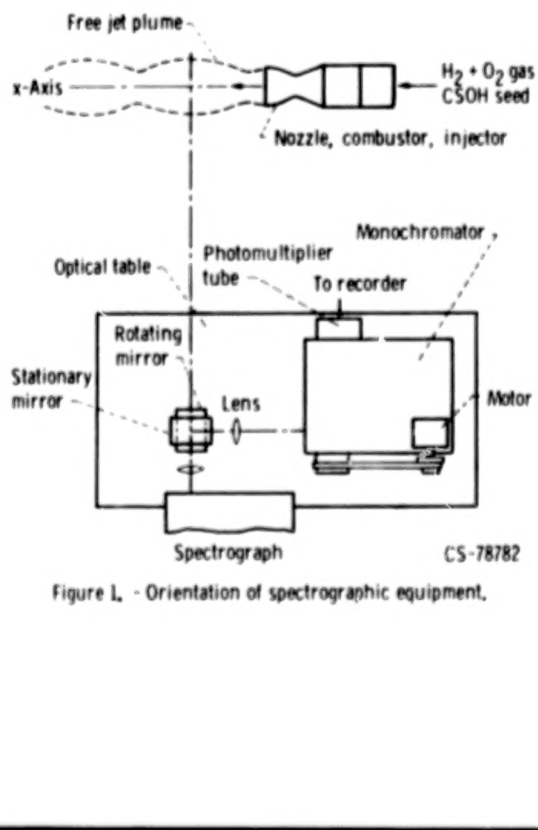

Figure 1. - Orientation of spectrographic equipment.

base in such a fashion as to be also inclined at a 45° angle to both the optical and vertical axes. Thus, in traversing the mirror system, the radiation undergoes two 90° rotations, one about the vertical axis and one about the optical axes. Thus, the plasma image is focused on the spectrometer entrance slit such that the plasma x-axis is parallel to the slit. With reference to figure 2, the slab of plasma with radiant intensity Q_y therefore has a width Δy defined by the spectrometer slit width. A fishtail diaphragm at the entrance slit is used to define the plasma length Δx irradiating the spectrometer optics.

The rotating-mirror platform scans the plasma image across the slit and thereby provides a transverse profile $Q_y(y)$. The photomultiplier response to this transverse scan is recorded on both a memory oscilloscope and the high speed visicorder. System

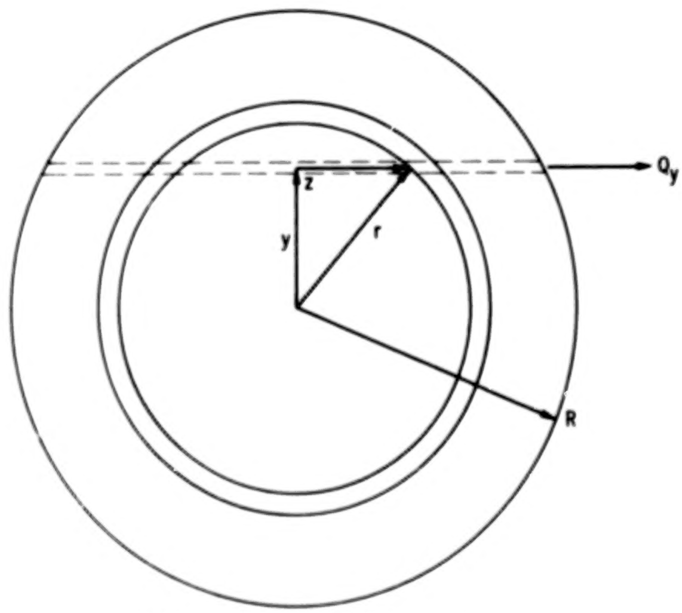

(a) Cross section of cylindrical plasma column.

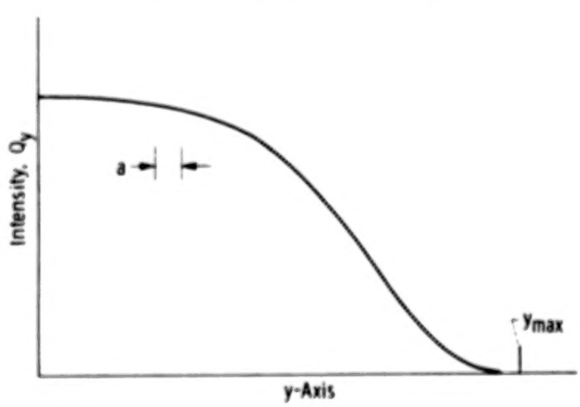

(b) Transverse profile of intensity.

Figure 2. - Plasma profile.

calibration for absolute intensity measurements is accomplished with a tungsten ribbon filament lamp mounted in place of the plasma on the plasma axis.

Spectrometer entrance slit widths are characteristically 30 to 60 micrometers, with corresponding exit slit widths being 600 to 1200 micrometers.

SPECTROSCOPIC METHOD

A gas is said to be in a condition of local thermodynamic equilibrium (LTE) when the electrons, atoms, molecules, and ions are in equilibrium with themselves, but not with the photons. In order that the plasma be in LTE, it is necessary that the collisional rates which populate and depopulate the various energy levels of the plasma species exceed the corresponding radiative rates. Cool (ref. 2) has shown that LTE exists in an atmospheric potassium-seeded plasma for an electron temperature of 2500 K and an electron number density of 10^{14} per cubic centimeter. In this case the rates of radiative deexcitation and recombination were well below that of electron collisional deexcitation and recombination. These conditions approximately represent the conditions of the present experiment, except that the major plasma constituent is water vapor rather than air. However, the radiative/collisional rate ratio for water is less than for air, thereby further justifying the assumption that the present plasma is in LTE.

Line emission is determined by bound-bound transitions between upper level m and lower level n. The radiated power per unit volume, per unit solid angle, and per unit wavelength interval is (ref. 3)

$$\epsilon_\lambda = \frac{hc}{4\pi\lambda_0} L_\lambda A_{nm} N_m \tag{1}$$

where L_λ is taken to be the normalized Lorentz profile from reference 4:

$$L_\lambda = \frac{2W_{1/2}/\pi}{4(\lambda - \lambda_0)^2 + W_{1/2}^2} \tag{2}$$

for a line center at λ_0 with halfwidth $W_{1/2}$, A_{nm} is the transition probability between lower level n and upper level m, and N_m is the number of density at upper level m related to the total number density N_{sn} of neutral cesium atoms by the Boltzmann relation

$$N_m = N_{sn} \frac{g_m}{Z_s} \exp\left(\frac{-E_m}{kT}\right) \tag{3}$$

Relating the transition probability A_{nm} and the absorption oscillator strength f_{mn} by

$$A_{nm} = \frac{8\pi^2 r_0 c}{\lambda_0^2} \frac{g_n}{g_m} f_{mn} \tag{4}$$

gives the emission coefficient radiated over the bandwidth $\Delta\lambda$ of a spectral line as

$$Q_r = \int_{\Delta\lambda} \epsilon_\lambda \, d\lambda = \frac{2\pi h r_0 c^2}{Z_s} \frac{g_n f_{mn} N_{sn} F}{\lambda_0^3} \exp\left(\frac{-E_m}{kT}\right) \tag{5}$$

where

$$F \equiv \frac{\int_{\Delta\lambda} \epsilon_\lambda \, d\lambda}{\int_0^\infty \epsilon_\lambda \, d\lambda} \tag{6}$$

The function F is plotted in reference 5 as a function of the volumetric absorption coefficient $\rho K\nu$ and the ratio of bandwidth to halfwidth $\Delta\lambda/W_{1/2}$ and is approximately equal to one for the present experiment. The number density of neutral cesium atoms N_{sn}, obtained from the ideal gas law, is given by

$$N_{sn} = 7.24\times10^{22} \frac{pS}{T} \tag{7}$$

where p is the gas pressure in pascals, T the temperature in kelvins, and S the mole fraction of neutral cesium atoms as calculated by a chemical equilibrium composition program (ref. 6). Values of the energy of the upper state E_m, the statistical weight at the lower state g_n, and the oscillator strength f_{mn} are found in references 7 and 8.

ABSOLUTE INTENSITY CALIBRATION

As mentioned previously, the optical system is calibrated using a tungsten ribbon filament lamp mounted such that the filament is on the plasma axis. With the spectometer set at the wavelength of the cesium lines, a series of measurements are made at increasing filament brightness; each measurement consists of a photomultiplier signal voltage and a filament brightness temperature determined with an optical pyrometer.

It is desired to formulate a spectrometric calibration function which will relate the photomultiplier signal voltage V_{pm} to Q_s, the radiant power flux per unit solid angle within the bandwidth $\Delta\lambda$ of the spectrometer at the test wavelength λ_t. Recognizing that for calibration purposes the test radiation is rising from the tungsten filament, Q_s is given by

$$Q_s(\lambda_t) = \tau(\lambda_t)\epsilon(\lambda_t, T_t)Q_p(\lambda_t, T_t)\Delta\lambda \tag{8}$$

where $\tau(\lambda_t)$ is the transmittance of the lamp glass envelope, $\epsilon(\lambda_t, T_t)$ the spectral emissivity of the tungsten filament, $Q_p(\lambda_t, T_t)$ the Wien form of the blackbody radiation function, and $\Delta\lambda$ the bandwidth of the spectrometer.

The true temperature T_t of the tungsten filament is obtained from its brightness temperature T_b, observed by a pyrometer of effective wavelength λ_p. Since the pyrometer is calibrated in terms of a blackbody, it follows that

$$Q_p(\lambda_p, T_b) = \tau(\lambda_p)\epsilon(\lambda_p, T_t)Q_p(\lambda_p, T_t) \tag{9}$$

from which it follows that

$$\frac{1}{T_t} = \frac{1}{T_b} + \frac{\lambda_b}{C_4} \ln[\tau(\lambda_p)\epsilon(\lambda_p, T_t)] \tag{10}$$

Thus, from equations (8) and (10) values of Q_s are obtained for each brightness temperature measurement which, together with the corresponding V_{pm} values, yields the desired spectrometric calibration function by a least squares fit in the form

$$Q_s(\lambda_t) = c_0 + c_1V_{pm} + c_2V_{pm}^2 + c_3V_{pm}^3 \tag{11}$$

ABEL INVERSION

Generally 18 to 32 data points (Q_y, y) are obtained from a transverse scan of a plasma profile (fig. 2(a)). Following the method of Cremers and Birkebak (ref. 9), these data are divided into three zones and a least square fourth-degree polynomial is fitted to each zone. The zones overlap one another by four data points, and the criterion for selection of the intersection between the zones is based on which intersection yields the best fit to the data.

Analytically, the Abel transformation of Q_y to radial emission coefficients Q_r is accomplished by the relation

$$Q_r = -\frac{1}{\pi}\int_r^R \frac{dQ_y/dy}{\left(y^2 - r^2\right)^{1/2}}\,dy \tag{12}$$

For digital computer processing, however, the numerical technique of Nester and Olsen (ref. 10) is employed. In this technique both the radius and the y-axis are divided into increments "a" such that

$$r_k = ka \tag{13}$$

$$y_n = na \tag{14}$$

and

$$y_{max} = Na \tag{15}$$

where y_{max} is the value of y where $Q_y = 0$ as shown in figure 2(b). From the geometry of the inversion process shown in figure 2(a), it is seen that y_{max} is numerically equal to R.

With these identifications, equation (12) may be manipulated into the form

$$Q_k = -\frac{2}{\pi a}\sum_{n=k}^{N} B_{k,n}Q_n \tag{16}$$

where

$$Q_k = Q_r \qquad r = ka$$

$$Q_n = Q_y \qquad y = na$$

$$B_{k,n} = -D_{k,k} \qquad n = k$$

$$B_{k,n} = D_{k,n-1} - D_{k,n} \qquad n \geq k + 1$$

$$D_{k,n} = \frac{\left[(n+1)^2 - k^2\right]^{1/2} - \left(n^2 - k^2\right)^{1/2}}{2n + 1}$$

TEMPERATURE PROFILE RATIOCINATION

From equations (5) and (7) it can be seen that the emission coefficient is functionally dependent on temperature, plasma static pressure, and the mole fraction of neutral cesium atoms:

$$Q(r) \sim \frac{p(r)S(r)}{T(r)} \exp\left[\frac{-E_m}{kT(r)}\right]$$

Obviously, the radial temperature profile can be determined from $Q(r)$ only if $p(r)$ and $S(r)$ are known from other sources. For this work, $p(r)$ was obtained from a two-dimensional supersonic free jet computer program which uses the method of characteristics (ref. 11 and private communication with A. R. Bishop, NASA Lewis Research Center) to relate pressure to temperature, input composition, and nozzle geometry. $S(r)$ was obtained from a chemical equilibrium program (ref. 6) which thermodynamically relates $S(r)$ to $T(r)$ and input composition. The relations $p_r(T_r$, composition, geometry), $S_r(T_r$, composition), and $Q_r(T_r, p_r, S_r)$ were iteratively solved for that T_r yielding a self-consistent solution.

RESULTS AND DISCUSSION

A set of profiles in sequence of integrated intensity, emission coefficient, pressure, and temperature is shown in figures 3 to 6, respectively, for combustion chamber pres-

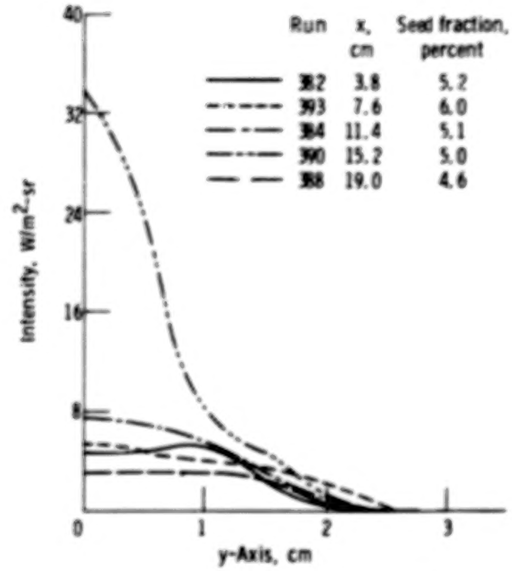

Figure 3. - Integrated intensity as function of y-axis at combustion pressure of 10^6 newtons per square meter.

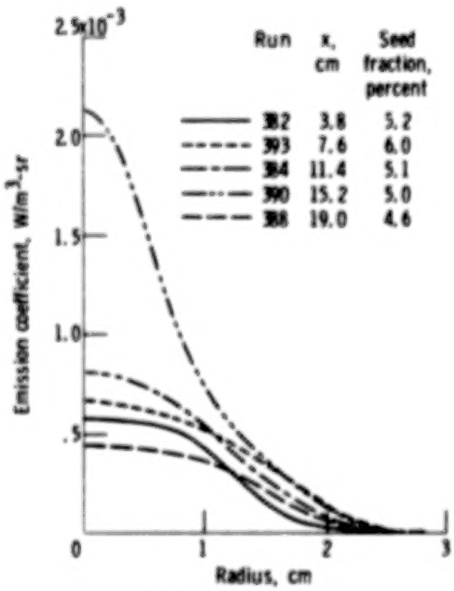

Figure 4. - Emission coefficient as function of radius at combustion pressure of 10^6 newtons per square meter.

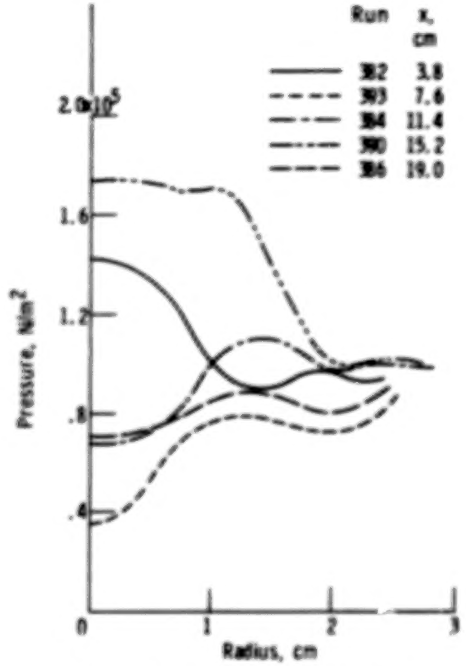

Figure 5. - Pressure as function of radius at combustion pressure of 10^5 newtons per square meter.

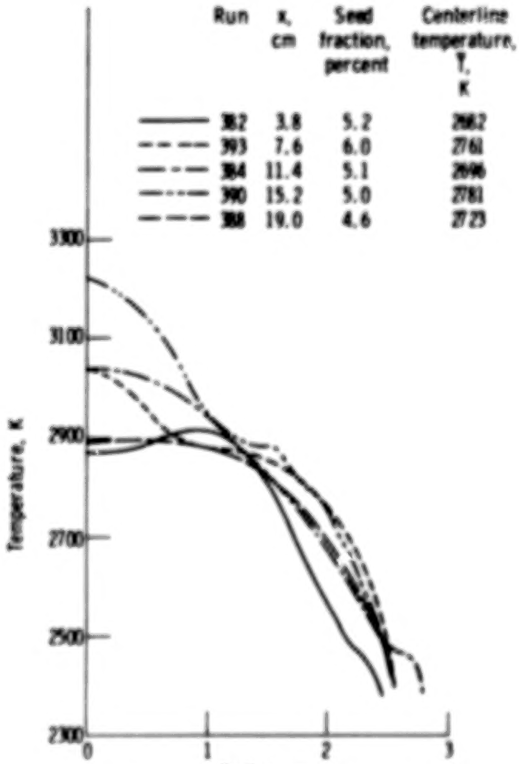

Figure 6. - Temperature as function of radius at combustion pressure of 10^5 newtons per square meter.

sure of 1.0 megapascal. Each figure contains five curves representing data taken at different axial positions downstream of the nozzle exit. The plume nodes occur at positions 3.8 and 19.0 centimeters, approximately. The shapes of the temperature profiles in figure 6 reveal the inherent effects of compression and expansion pressure waves characteristic of a supersonic free jet. The centerline temperatures vary from about 2900 to 3200 K. The free boundary contour of the plasma plume has 2.4 to 2.8 centimeter radii as defined by a temperature of about 2400 K, below this the intensity is too small (<1.0 W/m^2 - sr) to record.

The effect on the temperature profile of lowering the chamber pressure from 1.0 to 0.5 megapascal is shown in figure 7. The profile is generally steeper and the plume size is smaller (radii, 1.8 to 2.1 cm). The corresponding pressure profile is shown in

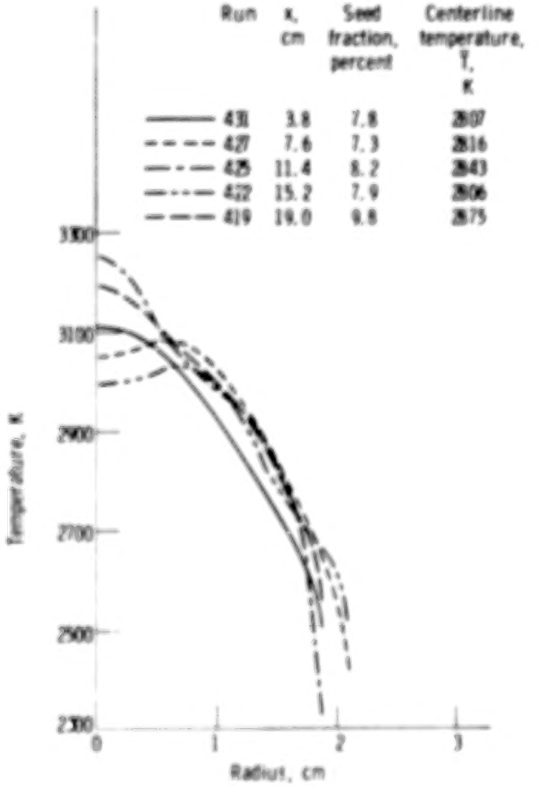

Figure 7. - Temperature as function of radius at combustion pressure of 5x10^5 newtons per square meter.

figure 8. Raising the chamber pressure to 2.0 megapascals results in the plume radii increasing to 2.7 to 3.7 centimeters, as shown in figure 9, while some of the temperature profiles decrease from their maximum of about 3000 K to approximately 2600 K at the centerline. The corresponding pressure profile is shown in figure 10.

The effect of seed fraction can be seen from figure 11 for the same chamber pressure and axial position. The rate of change of peak intensity decreases with increasing seed fraction.

Temperature profiles were also measured for some of the previous operating conditions using the CsI 0.5636-micrometer transition. One such typical measurement is shown in figure 12. On the average, temperature measurement using the 0.5636-micrometer line agree to within 4 percent with those obtained using the 0.5664-micrometer line.

The experimental uncertainty in temperature due to intensity measurement, data reduction, and calibration procedures is estimated to be about 5 percent.

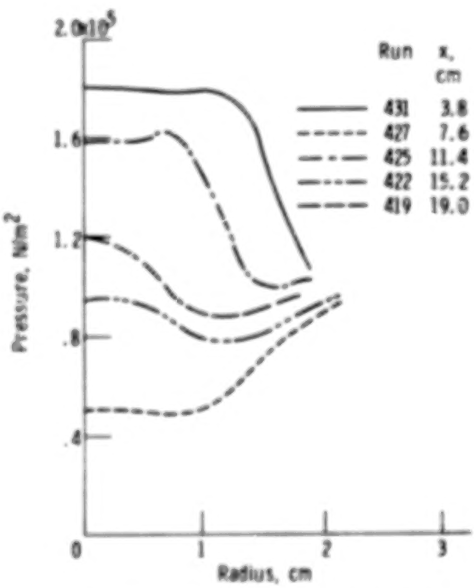

Figure 8. - Pressure as function of radius at combustion pressure of 5x10^5 newtons per square meter.

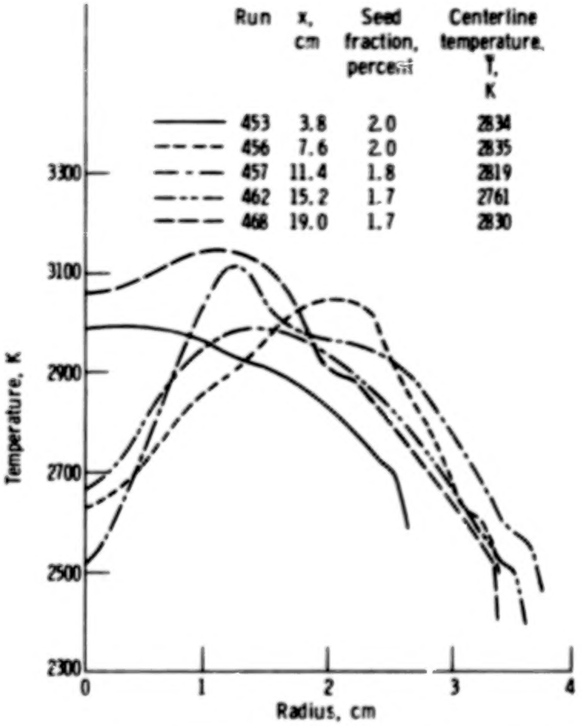

Figure 9. - Temperature as function of radius at combustion pressure of $2x10^6$ newtons per square meter.

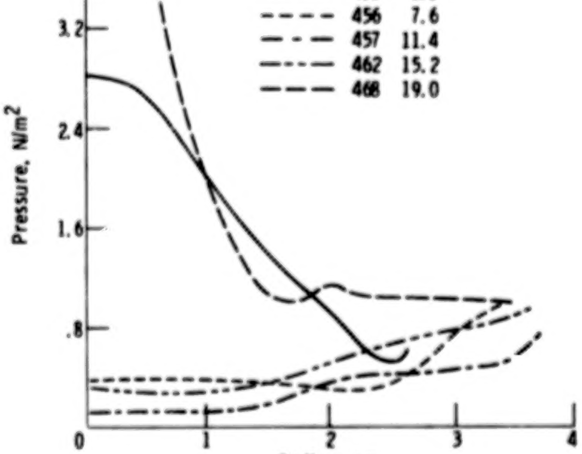

Figure 10. - Pressure as function of radius at combustion pressure of $2x10^6$ newtons per square meter.

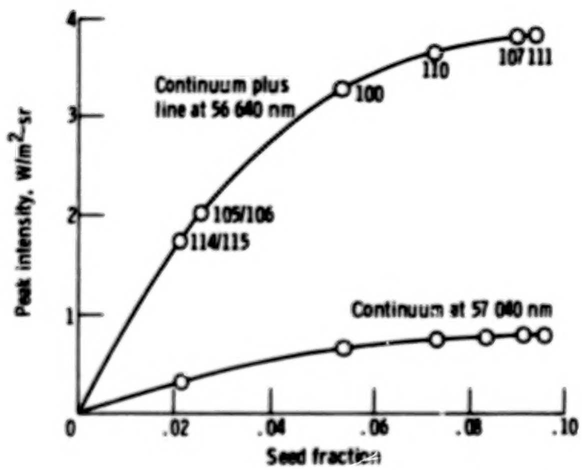

Figure 11. - Peak intensity as function of seed fraction at combustion pressure of 10^6 newtons per square meter and x = 5.4 centimeters.

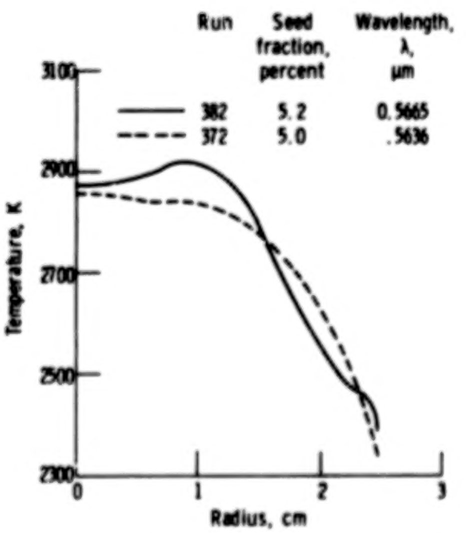

Figure 12. - Radial temperature profiles at 0.5664 and 0.5636 micrometer wavelengths, combustion pressure of 10^6 newtons per square meter, and x = 3.8 centimeters.

CONCLUDING REMARKS

Results of the spatially resolved temperatures have demonstrated the feasibility of the diagnostic technique of absolute intensity measurement for the seeded combustion plasma jet, if the density profile is known. The work provides a tool to study the thermal field of an axisymmetric MHD duct.

If the plasma were measured from side and top (i. e., at different angles in the plane perpendicular to the flow axis), the axisymmetry would be better assessed.

The reader may ask why temperature was not measured using a two lines method so that density might be determined using $T(r)$ as the independently measured quantity. This was tried, but the fluctuations in the temperatures so obtained were intolerably large. These fluctuations may have arisen from two sources: (1) the errors in the Abel inversion technique, or (2) the fact that sequential rather than simultaneous scans were measured due to instrumental limitations. The failure of this initial approach dictated the development of the semi-theoretical approach herein described.

Lewis Research Center,
National Aeronautics and Space Administration,
Cleveland, Ohio, November
506-25.

APPENDIX A

METHOD FOR ESTIMATION OF THE OPTICAL THICKNESS

The optical thickness estimation has been reported before (refs. 12 and 13) by calculating the volumetric absorption coefficient:

$$\rho K\nu = \frac{e^2}{2\pi\epsilon_0 m_e c^2} \frac{f_{mn}}{\Delta\nu_c} \frac{g_n}{g_0} N_{sn} \exp\left(\frac{-E_n}{kT}\right) \tag{A1}$$

where the line halfwidth is dominated by Lorentz broadening. This pressure broadening by different gas particles is given in references 14 and 15 by

$$\Delta\nu_c = \frac{2}{\pi} Q_{opt} N_g \sqrt{2\pi\bar{R}T\left(\frac{1}{M_{sn}} + \frac{1}{M_g}\right)} \tag{A2}$$

An experimental value for the optical cross section Q_{opt} of the CsI 0.8521-micrometer line is given in reference 15 in the form $Q_{opt}/T_g^{1/5}$. The optical cross sections of other CsI lines can be obtained from this using the following relation from reference 16:

$$\frac{Q_{opt}}{Q_{opt\ 0.8521\ \mu m}} = \frac{C^{2/5}}{C^{2/5}_{0.8521\ \mu m}} = \frac{\left(r_i^2 - r_f^2\right)^{2/5}}{\left(r_i^2 - r_f^2\right)^{2/5}_{0.8521\ \mu m}} \tag{A3}$$

where C is the van der Waals constant of interaction. The quantum mechanical average of the square of the so-called "radius" of the initial (α = i) and final (α = f) energy states is given in reference 3 as

$$\overline{r_\alpha^2} = \frac{a_0^2}{2}\left(\frac{E_H}{E_\infty - E_\alpha}\right)\left[5\left(\frac{E_H}{E_\infty - E_\alpha}\right) + 1 - 3l_\alpha(l_\alpha + 1)\right] \tag{A4}$$

where E_H = 13.595 electron volts, E_∞ = 3.893 electron volts, and l_α is the orbital quantum number of the state i or f.

For a gas temperature of 3000 K, the cross sections of the CsI, 0.5664 and 0.5636

micrometer lines are 6.2 and 7.9 square nanometers, respectively. For $S_f = 0.001$, $\rho K\nu \leq 0.15$ per centimeter for both lines, which are considered approximately optically thin.

APPENDIX B

SYMBOLS

A_{nm}	transition probability
a_0	constant (ref. 3, p. 99), first Bohr radius, 0.52917 Å
$B_{k,n}$	defined in ref. 9
C	Van der Waals constant
c	speed of light
c_0, c_1, c_2, c_3	defined by eq. (11)
c_4	1.44×10^{-2} (m)-(K)
$D_{k,k}, D_{k,n}, D_{k,n-1}$	defined by eqs. (14) to (16)
E_H, E_∞	first ionization potentials of H and Cs atoms, respectively
E_m	energy of upper level
e	electron charge
F	ratio of spectral line energy in bandwidth $\Delta\lambda$ to total spectral line energy
f_{mn}	absorption oscillation strength
g_m, g_n	statistical weight of upper and lower state
g_0	statistical weight of ground state
h	Planck's constant
k	Boltzman's constant
L_λ	Lorentz broadening spectral line profile
l_α	orbital quantum number of state α
M_g	molecular weight of gas
M_{sn}	atomic weight of Cs seed
m_e	electron mass
N_g	number density of gas particles
N_m	number density of Cs atoms at upper level
N_{sn}	number density of neutral Cs atoms
p	pressure

Q_{opt}	optical cross section
Q_p	Planck function
Q_r	emission coefficient
Q_s	defined by eq. (8)
Q_y	integrated intensity
R	radius
$\overline{R}$	universal gas constant
r_0	classical radius of electron
$\overline{r_i^2}, \overline{r_f^2}$	square of classical electron radius of states i and f
S_f	mole fraction of neutral Cs atoms
T	temperature
T_b	brightness temperature
T_t	true temperature
V_{pm}	photomultiplier tube voltage output
$W_{1/2}$	spectral line width at half height
x	axial position downstream of nozzle exit
y	axis perpendicular to x
Z_s	partition function of Cs atom (=2)
ϵ_λ	emission coefficient
λ_0	wavelength at line center
λ_p	effective wavelength of pyrometer
$\Delta\lambda$	bandwidth
$\rho K\nu$	volumetric absorption coefficient
τ	transmittance
$\Delta\nu_c$	collisional broadening halfwidth in wave numbers

REFERENCES

1. Smith, J. M.: Results and Progress on the NASA Lewis H_2-O_2 MHD Program. 15th Symposium on the Engineering Aspects of Magnetohydrodynamics, Pennsylvania Univ., 1976, pp. IX.2-IX.6.

2. Cool, Terrill Alan: Recombination, Ionization, and Nonequilibrium Electrical Conductivity in Seeded Plasmas. Ph.D. Thesis, California Institute of Technology, 1965.

3. Griem, Hans R.: Plasma Spectroscopy. McGraw-Hill Book Co., Inc., 1964, p. 99.

4. Mitchner, M., and Kruger, Charles H., Jr.: Partially Ionized Gases. John Wiley & Sons, Inc., 1973.

5. Morris, J. C.; Krey, R. U.; and Garrison, R. L.: Radiation Studies of Arc Heated Nitrogen, Oxygen, and Argon Plasmas. Tech. Rep., 1 June 1965-15 June 1967, Avco Corp., 1968. (AFARL-68-0103, AD-676651.)

6. Gordon, Sanford; and McBride, Bonnie J.: Computer Program for Calculations of Complex Chemical Equilibrium Compositions, Rocket Performance, Incident and Reflected Shocks, and Chapman-Jouquet Detonations. NASA SP-273, 1967.

7. Agnew, L.; and Summers, C.: Quantitative Spectroscopy of Cesium Plasmas. Proceedings of the 7th International Conference on Phenomena in Ionized Gases, Vol. II, B. Perovic and D. Tosic, eds., Boris Kidric Inst. Nuclear Sciences (Giograd), 1966, pp. 574-580.

8. Moore, Charlotte E.: Atomic Energy Levels as Derived from the Analyses of Optical Spectra. NSRDS-NBS 35, Vol. 3, National Bureau Standards, 1971.

9. Cremers, Clifford J.; and Birkebak, Richard C.: Application of the Abel Integral Equation to Spectrographic Data. Appl. Opt., vol. 5, no. 6, June 1966, pp. 1057-1064.

10. Nester, O. H.; and Olsen, H. N.: Numerical Methods for Reducing Line and Surface Probe Data. SIAM Rev., vol. 2, no. 3, July 1960, pp. 200-207.

11. Hayes, Wallace D.; and Probstein, Ronald F.: Applied Mathematics and Mechanics. Vol. 5, Hypersonic Flow Theory, Academic Press, 1959, chap. 7.1.

12. Wang, S. Y.; and Benenson, D. M.: Radial Distribution of Electron and Gas Temperatures in a Potassium-Seeded Argon Plasma. International Conference on Plasma Science, IEEE, 1976, Session 2B11, p. 49.

13. Wang, Shih-Ying: Experimental Investigation of a Potassium-Seeded Argon Plasma. Ph.D. Thesis, State Univ. of New York at Buffalo, 1975.

14. Mitchell, Allan C. G.; and Zemansky, Mark W.: Resonance Radiation and Excited Atoms. Univ. Press, Cambridge, 1961, p. 170.

15. Hiramoto, Tatsumi: Rates of Total and Local Radiative Energy Losses in Non-equilibrium Plasmas. J. Phys. Soc. Jpn., vol. 26, no. 3, Mar. 1969, pp. 785-801.

16. McGregor, Douglas David: Electronic Nonequilibrium in a Supersonic Expansion of Ionized Gas. Appendix M, Optical Cross Sections for the 5P-3D Transition. SU-IPR-474, Stanford Univ., 1962, pp. 247-248. (AFOSR-72-2049TR, AD-750943.)

1. Report No.	2. Government Accession No.	3. Recipient's Catalog No.
NASA TP 1162		

4. Title and Subtitle	5. Report Date
TEMPERATURE DISTRIBUTIONS OF A CESIUM-SEEDED HYDROGEN-OXYGEN SUPERSONIC FREE JET	February 1978
	6. Performing Organization Code
7. Author(s)	8. Performing Organization Report No.
Shih-Ying Wang and J. Marlin Smith	E-9267
9. Performing Organization Name and Address	10. Work Unit No.
National Aeronautics and Space Administration Lewis Research Center Cleveland, Ohio 44135	506-25
	11. Contract or Grant No.
	13. Type of Report and Period Covered
12. Sponsoring Agency Name and Address	Technical Paper
National Aeronautics and Space Administration Washington, D. C. 20546	14. Sponsoring Agency Code

15. Supplementary Notes

16. Abstract

Radial distributions of temperature were determined spectroscopically in a Cs-seeded, H_2-O_2 plasma jet. The plasma was generated at combustion chamber pressures ranging from 0.5 to 2.0 megapascals and for various seed ratios (1 to 10 percent). The plasma was observed as the atmospheric exhaust from a NASA Lewis Mach 2 rocket test facility. Transverse profiles of the absolute integrated intensity were measured with the optically thin CsI lines (0.5664 and 0.5636 μm) at a range of axial positions downstream of the 5-cm-diam combustor-nozzle exit. Radial profiles of the emission coefficient were obtained from the measured transverse profiles of intensity by Abel inversion. Temperatures were then determined from the emission coefficients for conditions of local thermodynamic equilibrium using particle densities generated by a two-dimensional free jet computer program. Temperature results show the inherent effects of compression and expansion pressure waves characteristic of a free jet exiting from a supersonic nozzle.

17. Key Words (Suggested by Author(s))	18. Distribution Statement
Plasma physics Spectroscopy	Unclassified - unlimited STAR Category 75

19. Security Classif. (of this report)	20. Security Classif. (of this page)	21. No. of Pages	22. Price*
Unclassified	Unclassified	22	

* For sale by the National Technical Information Service, Springfield, Virginia 22161

NASA-Langley, 1978